J-Researchers

JOURNAL OF CIVIL ENGINEERING RESEARCHERS

Investigation and comparison of four new types of damper

Vatani A.,[a] Sadeghian S.,[b]

[a]*First affiliation,Assistant Professor, Engineering faculty, Chalous Branch, Islamic Azad University, Chalous, Iran*

[b]*Second affiliation, Junior, Faculty of Engineering,* Chalous *Branch, Islamic Azad University,* Chalous*, Iran*

Journals-Researchers use only: Received date here; revised date here; accepted date here

Abstract

The unfavorable experience of the past earthquakes and their respective financial and human loss indicates the weak seismic performance of some buildings. Hence, employing new equipment and tools is inevitable in this respect. The first idea is a multi-level passive control system able to shift the dynamic behavior parameters such as stiffness, strength, and damping ratio to absorb the seismic energy on multiple levels. This system is made up of a combination of nested pipe components absorbing energy during moderate and intense earthquakes. The second idea of the paper constitutes a new metal slit damper made of metal plates with high elevation whose metal parts are connected. The weak slit damper part is designed to work during low to moderate seismic induction, while the strong slit damper section is designed to be activated during large earthquakes. Another study examines the seismic behavior of a new type of damper consisting of U-shaped steel plates as energy-dissipating elements empirically, and the last study explores the performance of U-shaped yielding steel dampers in steel building frames. The present paper reviews and compares four types of introduced dampers.

"Keywords:Ductility; damper; Nonlinear dynamic analysis; U-shaped damper; Hysteretic dampers; Multi-level control system"

1. Introduction

The unfavorable experience of the pas earthquakes and their respective financial and human loss indicates the weak seismic performance of some buildings and the necessity of employing new equipment in this regard. Using metal dampers is among the practical and effective ways of promoting constructions' seismic performance. The prevalent seismic design of building structures is based on the inelastic behavior of some construction elements in the face of seismic energy input. Dampers can concentrate the input energy dissipation in pre-determined areas and prevent inelastic behaviors in gravity bearing primary construction elements. The benefits of seismic dampers have long been known to improve systems' seismic performance. Historical reviews of relative works can be found in other places. Seismic dampers have been proposed based on various mechanisms (for instance, energy depreciation through friction, metal yield, and the use of viscous, viscoelastic, or smart materials) and gradually became common in many structures all around the world. Seismic dampers depreciating

energy through steel yield are known to be among the most popular alternatives in the seismic engineering community due to their relatively low costs, easy analysis, modeling, design and installation, stiffness and strength adjustment, and stable performance and durability under the temperature changes in the workplace.

Yielding steel dampers and friction dampers are two effective systems in energy depreciation. The idea of employing steel energy depreciators to absorb the seismic energy in constructions emerged with the empirical and conceptual works of Kelly[1] and Skinner[2]. They proposed and examined various simple metal devices as energy-dissipating tools one of which were U-shaped metal strips. The reversible load test results revealed that U-shaped metal strips could work through large displacements in the inelastic range and depreciate energy through steel deformation. Another type of these devices is Added Damping and Stiffness (ADAS) elements designed to dissipate seismic energy through soft steel plates' flexural yield deformation[3]. After a couple of years, U-shaped elements' energy absorption and dissipation qualities were examined and confirmed by another group of researchers through performing through a series of cyclic testing in 1992[4]. Supplementary studies regarding these types of damper were conducted by Dolce[5] to make them functional. He performed numeral and empirical examinations on a circular arrangement of U-shaped strips as an elastoplastic biaxial device aimed at the passive control of structures.

Using double-level or multi-level control systems are among the new techniques that have attracted the attention of scholars over recent years. The main idea behind these systems is a combination of various control systems with different stiffness and strengths which brings about optimal energy dissipation on various seismic levels. Balendra et al.[6] proposed a two-level passive control system made up of a knee brace and perforated web plate connections. In low force and service loadings, the slit connection dissipates energy through friction dissipation, while the energy dissipation in severe earthquakes is provided by the knee element's elastic behavior. Using a combination of knee elements and vertical connection beams, Zharai and Vosooq[7] conducted a study on dual systems. The plastic hinge located on the vertical connection promotes energy dissipation under low forces, and the plastic knee brace deformation promotes ductility and energy absorption under intense forces, resulting in improved seismic performance.

2. Examination of the proposed models

The first damper under study has been proposed by Cheraghi and Zahrai[8]. As Figure 1 indicates, two pistons are designed inside the external pipe, connecting the external and internal pipes. Piston head displacements engage the internal and external pipes under tensile and compressive forces, generating a compound function. Stiffeners are also placed in both pipe directions to restrict the concentration of pipes' local buckling.

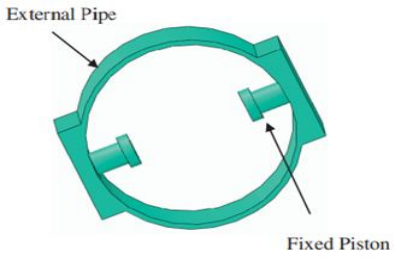

Figure 1: external pipe details

As indicated in Figure 2, the cylinders are installed outside of the internal pipe so that all parts of the pipe remain connected. The fixed piston moves within the cylinder and causes a compound compression and docility function. Figure 3 illustrates the assembled proposed damper.

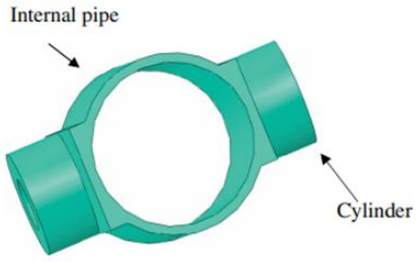

Figure 2: internal pipe details

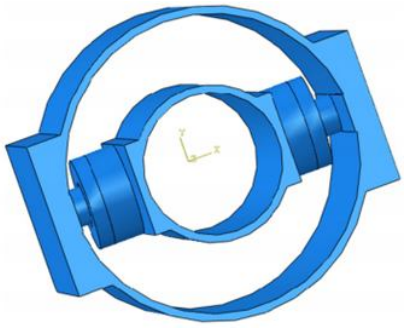

Figure 3: the assembled proposed damper

A cross-section is indicated in Figure 4 to manifest the mechanism of the proposed damper. The cross-section of the two pipes are initially completely independent, and only the external pipe's flexural strength resists against the forces applied. Then, as the displacement and force increase, the internal and external pipes become engaged and increase the strength and stiffness due to their compound function

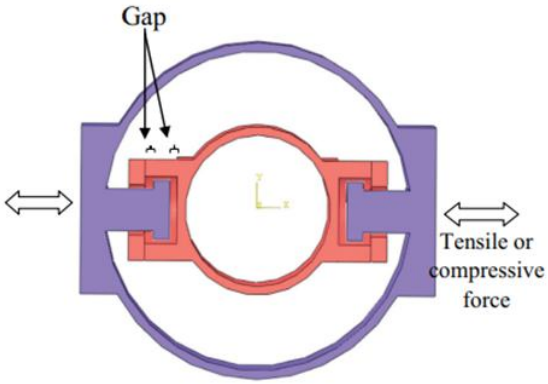

Figure 4: damper cross-section illustrating the proposed mechanism

Naeem and Kim[9] have proposed a new energy dissipation device which depends on displacement to protect frame structures. The multi-slit damper (MSD) is constituted of a combination of weak and strong steel slit dampers in series. MSDs entail two energy dissipation stages with different stiffness and yield forces.

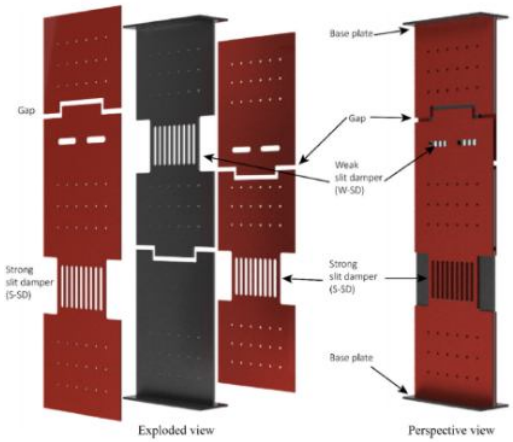

Figure 5: the separate parts of the multi-slit damper

The multi-slit proposed in this study is composed of three highly elevated metal plates screwed together as Figure 5 illustrates. The center of the slit damper plated is located between the two plates with strong dampers. The three metal plates are bound together by bolts located on the top, middle, and bottom of the plates, and only the central plate is connected to the top and bottom of the loaded framework beams. Every side-plate is divided by ∏-shaped slits on its top and bottom, acting as a stopper for deactivating the weak slit damper placed in the center plate and as a load transmitter for activating the two strong slit dampers in side plates when dislocation reaches a certain amount. As side location increases, even the central plate's slit becomes closed and the strong slit dampers area also deactivated to prevent breaks. In this stage, MSD acts as a metal plate shear wall.

The other examined damper has been proposed by Qu et al.[10] and consists of energy dissipation elements made of U-shaped steel plates. As illustrated, the U-shaped steel plates are composed of three parts: two flanges and a web plate. Assuming that t_p –the thickness of the U-shaped plate- is considerably smaller than R –the centerline radius of the web plate's semicircle, the U-shaped plate deformation induced by flange-to-flange movement in the longitudinal direction would be similar to that of a rope on a moving spool. Figure b6 indicates the optimal curvature change distribution along the U-shaped plate. As indicates, curves are generated

intermittently at web plate-flange intersections while the center of the web plate moves in curvature with no change.

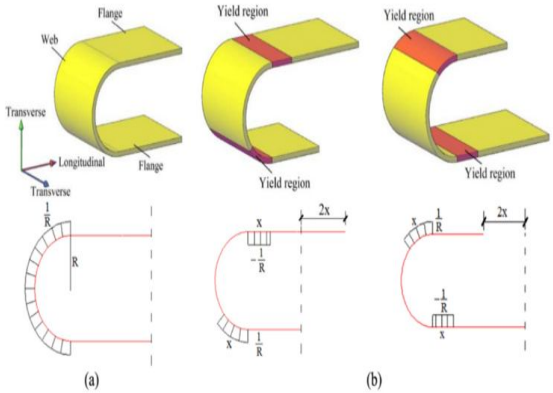

Figure 6: the optimal yield behavior of a U-shaped steel plate - a.The U-shaped plate and the initial curvature b. yield and curvature distribution in the U-shaped plate under cyclic displacement

Another study[10] proposes the damper illustrated in figure 7. As illustrated, the damper includes a series of symmetrically arranged U-shaped steel plates, two casing elements, diaphragm elements placed in regular intervals, and one piston element. The damper eliminates the energy through the flexural yield of the U-shaped steel plates under the cyclic longitudinal motion of the piston element. In the wake of an earthquake, casing elements and the piston element are exposed to the return of tension and pressure transmitted from the U-shaped steel plates. To achieve an optimally functioning damper, casing elements and the piston element must be designed in conformity with the capacity design model to prevent them from yielding under tension and buckling under pressure. The diaphragm elements are placed along the damper to reduce the unrestrained length of the piston element and side elements. The web plate of every diaphragm element has been slit to allow the passing of the piston element. The flanges of every diaphragm are connected to casing elements as well as two channels illustrated in Figure 7a. The open space between the adjacent diaphragm elements allows visual damage identification of the U-shaped metal plates post-earthquake and provides the possibility of proper substitution of the U-shaped steel plate after the earthquake, if necessary. It must be mentioned that the U-shaped steel plates had been proposed previously as energy-dissipation elements aiming to reduce the excess displacement responses of some of the structures detached from the ground[11].

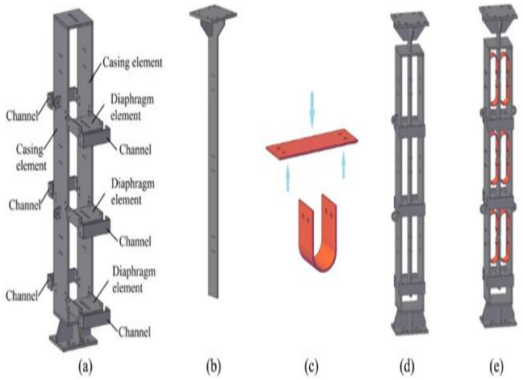

Figure 7: damper illustration a. casing and diaphragm elements b. piston element c. U-shaped steel plates' cold rolling process d. the damper before placing the U-shaped steel plates e. the damper after installing the U-shaped steel plates

Bagheri et al.[12] have developed a device for obtaining the U-shaped elements using cold rolled steel strips. In this device's uniaxial structure, the U-shaped element deforms along the direction parallel to the U-flanges (Figure 8). Besides, a circular arrangement similar to that of Figure 9 can be used to develop biaxial devices.

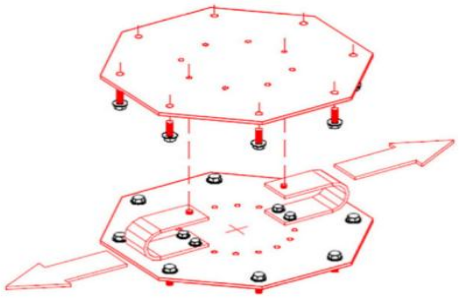

Figure 8: the U-shaped uniaxial yielding steel damper

Figure 9: the U-shaped biaxial yielding steel damper with a circular arrangement

In this paper[12], a pair of U-shaped elements are used a metal yielding damper as indicated in figure 8. This device is titled U1 and is composed of two U-shaped elements placed across from each other. It has been assumed that every section has a 10*100 mm profile and a curvature radius of 50 mm similar to the work of Dolce et al.[5]. To employ this type of damper in steel structure frames, it is suggested that top and bottom U-shaped element stripes be connected to or fixated on two horizontal plates. This device is connected from the top to the girder opening in a building frame and from the bottom to the inverted-V brace members.

3. Examination of the proposed models

To confirm the results, ensure the used parameters and characteristics in the numeral model, and determining the proximity to real conditions, Cheraghi et al.[8] have first designed a pipe with the external diameters of 220 mm, length of 100 mm, and thickness of 12 mm based on the modeling software and its outputs, and have then tested it under seismic loading[13]. Figure 10a indicates the comparison of the numeral and experimental results. Hysteresis cycles reveal a high ductility and effective energy absorption as well as conformity between numeral and experimental results.

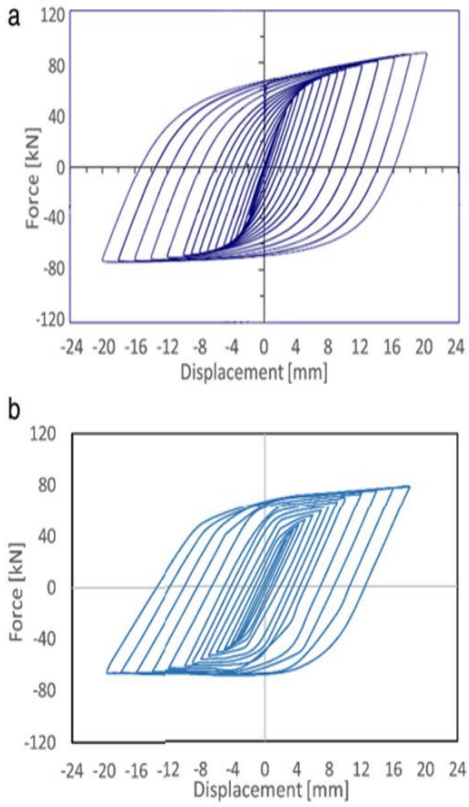

Figure 10: sample pipe Hysteresis curves: a. experimental model b. numeral model

Naeem et al.[9] have published the static loading test results conducted on a multi-slit damper (MSD) prototype on a full-scale. The loading test was conducted on the prototype with control on displacement since MSD is essentially a device dependent on displacement that dissipates seismic energy through yielding steel stripes. According to Coupen test results, the yielding tension of the steel used in this study on a multi-slit damper prototype made up of three steel plates with an experimental frame (2.913 mm) is illustrated in figure 11. Each steel plate has been vertically separated by the other with 30 mm intervals. The weak slit damper is placed on the tip of the central plate and two strong slit dampers are placed on the bottom of the two lateral plates. The damper has been designed to have initial yield strength of 50 kN (the weak slit section) in a

lateral displacement of 5.3 mm and a secondary yield strength of 122 kN (the strong slit section) in a displacement of 35 mm. the central plate and lateral plates are 20 mm and 15 mm thick, respectively. The slit beam length is weak and strong dampers is 270 mm and 230 mm, respectively.

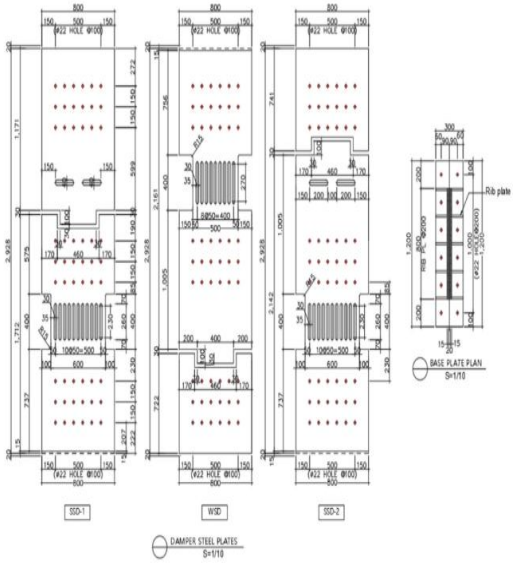

Figure 11: the dimensions of the multi-slit damper prototype

To examine the hysteretic behavior of the proposed damper, a cyclic loading with a controlled displacement MSD test was conducted using a self-propelled hydraulic actuator. Figure 12 indicates the force-displacement equation of the test sample obtained from the cyclic loading test. The weak slit damper yields first while the strong slit dampers remain elastic. When the weak slit damper's displacement reaches 30 mm which is slightly smaller than rupture displacement, the slits located between the side plates' top and bottom close, and the load is transmitted to the strong slit dampers in the bottom side plates while the weak damper restricts further deformation. Therefore, slit dampers prevent breaks and remain active through all seismic inductions. It has been observed that the weak slotted section first yields up to 5.3 mm, and then the load increases again so that strong slotted sections yield under displacement of 38 mm. figure 12 also indicates the dissipated energy, which means the area placed in the Hysteresis curve increases due to the increase in displacement since both slit dampers are active. The wastage curves are almost symmetric in both directions. The primary yield force of the weak slit damper equals 50 kN. However, the secondary yield point of the strong damper equals around 160 kN while its theoretical value has been estimated as 130 kN. This might be due to the engagement of a tension field across the steel plates during large displacements. The higher post-yield stiffness of the strong slit damper compared to the weak slit damper can also contribute to the aforementioned.

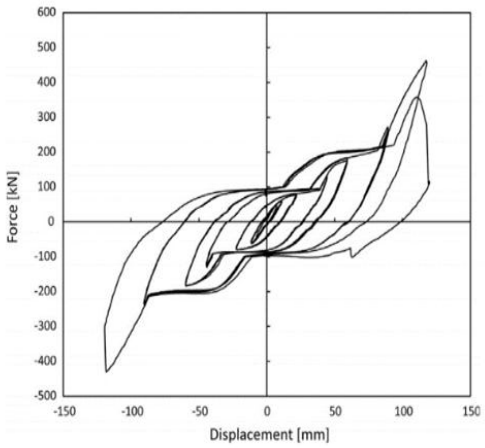

Figure 12: multi-slit damper Hysteresis Obtained from the loading test

The slit closure and the contact between the top and bottom plates are illustrated to be 1.5% of the relative displacement in Figure 13a, and the local distortion or deformation around the slits is illustrated to be 3% of the relative displacement in Figure 13b. Given the local deformation around the slit induced by the concentration of the large tension on the contact point, yield displacement changed in each loading cycle. The load transfer between the top and bottom plates in the loading cycle with 6% of the floor height ends when the relative deformations in top of the plate, bottom of the plate, and out of the plate becomes greater than the thickness of the plates. Figure 14 indicates the out-of-plane displacement between the top and bottom plates as well as the

permanent deformations of the slotted section during rupture. Figure 15 indicates the recorded strains measured by a strain gauge placed in the center of the strong slit damper. It can be observed in Figure 15a that the strong slit damper remains within the elastic range before reaching a 30 mm displacement which is equal to the slit distance. When the displacement grew larger than 38 mm, the strong slit damper yielded and the strain increased so that the slit in the central plate was closed, and the strong slit damper surrendered under around 90 mm displacement in one side. On the other side, the strain increased due to the local deformation around the plate slit until the displacement reached 120 mm. it can be observed from the recorded strains that considerable deformations have occurred in the slit damper which results in significant amounts of energy being dissipated.

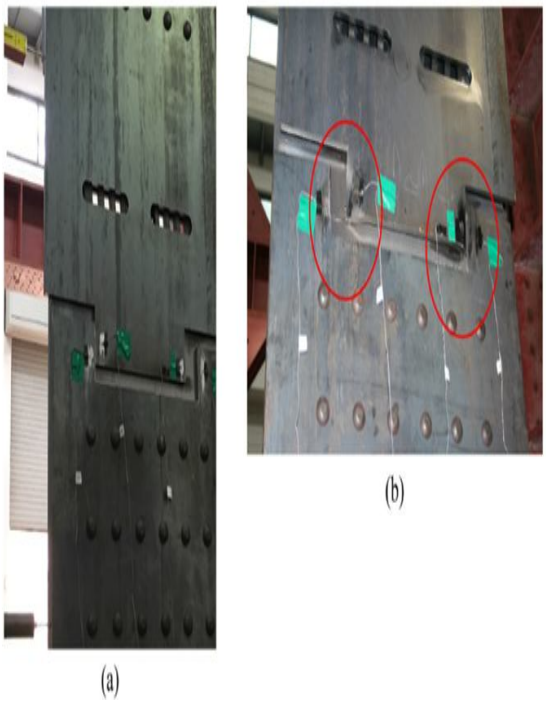

Figure 13: test sample deformation: a. slit closure, b. local deformation around the slit under 3% of the relative load

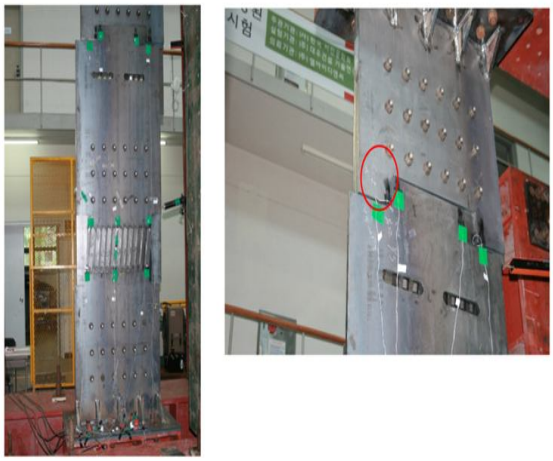

Figure 14: sample rupture state: a. permanent deformation in the slit section, b. displacement in the top and bottom plates and out-of-plane displacement

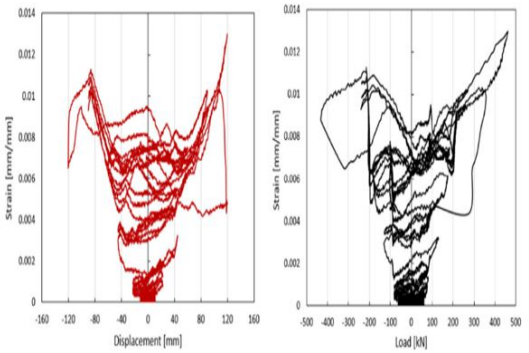

Figure 15: recordings from the strain gauge connected to one of the strong slit damper's steel stripes

It has been predicted that in the case of U-shaped dampers (Figure 10), the proposed damper will absorb the energy through U-shaped steel plates' flexural yield. As indicated in Figure 16, every sample includes 12 U-shaped steel plates. Two flanges of every U-shaped steel plate were respectively attached to one of the casing elements and the piston element using strong bolts. Test parameters including the geometry and properties of the U-shaped steel plates, and the shape of the holes made for strong bolts connecting the U-shaped steel plates to casing elements vary in samples A through G. figure 17 indicates the geometrical properties of

the U-shaped plates including their thickness (t_p), depth (D), height (H), flange width (W), and bolt hole dimensions (d and l). Table 1 also briefly illustrates the properties of the samples.

The U-shaped steel plates of samples A and B were similar. These two samples were tested using various loading protocols to examine the impact of loading protocols on the damper's seismic performance. Sample C and D U-shaped steel plates also had the same design as sample A, except they were 4mm and 12mm thick, respectively. Samples A, C, and D test results provided an opportunity to examine the impact of the U-shaped steel plates' thickness on damper strength. Sample E U-shaped steel plates were also similar to that of sample A, except that their flange width (w) was smaller. It is worth mentioning that when the flange-to-flange displacement becomes two times larger than flange width, the U-shaped steel plate's yield model will be different from what figure 1 illustrates. Sample E was tested to examine damper performance under displacements greater than twice the flange width. Samples A and F were made of U-shaped plates with similar geometries but different materials. Samples A and F test results help confirm whether the same behavior can be observed in U-shaped steel plates with the same geometrical properties but made out of different steels. Sample G U-shaped steel plates also resembled Sample A, except they had larger flange widths, and four of the 12 U-shaped steel plates were chosen to hold strong holes longitudinally, connecting the U-shaped steel plates to the casing elements in sample G.

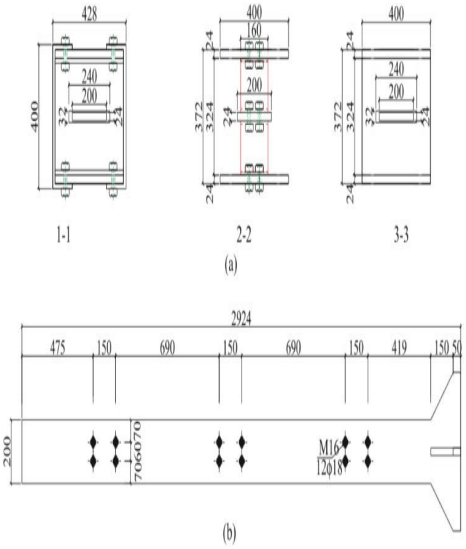

Figure 16: damper design: a. diaphragm and casing elements, b. piston element

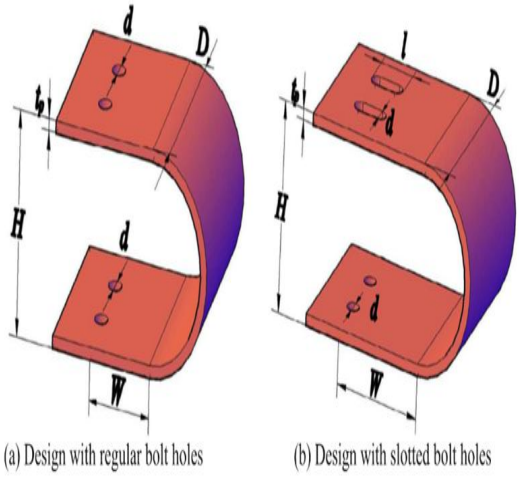

Figure 17: U-shaped steel plates' geometrical parameters: a. design with regular bolt holes, b. design with slotted bolt holes

Table 1
properties of every sample's U-shaped steel plates

Specimen ID	Geometries (mm)						Material	Mass[c] (kg)
	H	*D*	t_p	*W*	*d*	*l*		
A	150	160	8	80	18	-[a]	Q235B	4.84
B	150	160	8	80	18	-[a]	Q235B	4.84
C	150	160	4	80	18	-[a]	Q235B	2.32
D	150	160	12	80	18	-[a]	Q235B	7.61
E	150	160	8	50	18	-[a]	Q235B	4.25
F	150	160	8	80	18	-[a]	LY225	5.45
G[b]	150	160	8	120	18	48	Q235B	5.62

Generally, all samples showed stable hysteretic behaviors during the tests. No rupture in the samples' U-shaped steel plates was observed in phase 1 of the test, except for sample E. the yielding area length gradually grows along with the increase in displacement. Some considerable observations of sample E were made during the last four cycles of phase 1. As table 1 indicates, sample E had a smaller flange of 50mm; however, the maximum positive displacements imposed on sample E reached 108mm and 120mm in the final stage of phase 1. Therefore, the web plat centerline of every U-shaped steel plate in sample E did not remain round in the last four cycles of phase 1 due to the stretch and yield actions of the U-shaped steel plates concentrated on the transection consisting of bolt holes. Figure 18 indicates the deformed shape of sample E U-shaped steel plates under longitudinal displacements smaller and larger than twice the working flange width (which is 100mm). By the end of phase 1, visible ruptures were observed in sample E in slotted areas where the plate yield was concentrated.

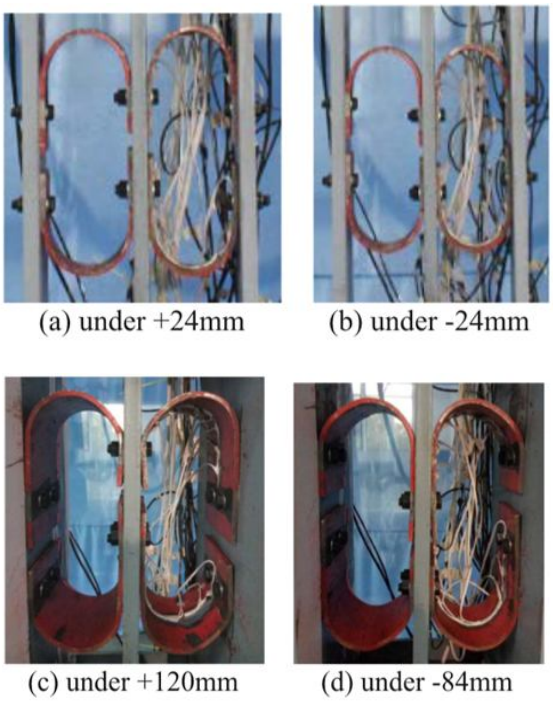

Figure 18: sample E U-shaped steel plates under various displacements

No visible rupture was observed in samples G and D over the second phase of the tests, while the U-shaped steel plates of other tested samples ruptured. In samples A and B, the ruptures began in the external surfaces where web plates and flanges met. These ruptures spread towards the inner parts of the U-shaped steel plates due to the gradual return of loading. By the end of phase 2, ruptures penetrated the depths of the plates but did not reach the full depth of the steel plates in the two aforementioned samples. Figure 19 indicates the rupture spread in the U-shaped steel plates of samples A and B. samples E and F also underwent ruptures in the depth of the U-shaped steel plates over the second phase of the test. As indicated in Figure 20, sample E has undergone ruptures in the thickness of the bolt holes, and the rupture has not penetrated the full depth of the U-shaped steel plates. As illustrated in Figure 21, sample F indicated ruptures both in thickness and the

depth of web plate-flange intersections of some U-shaped steel plates.

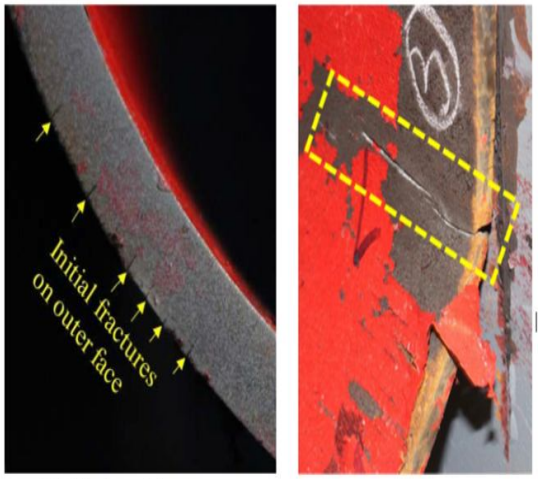

Figure 19: the typical ruptures in samples A and B: a. start of the rupture, b. typical ruptures by the end of the test

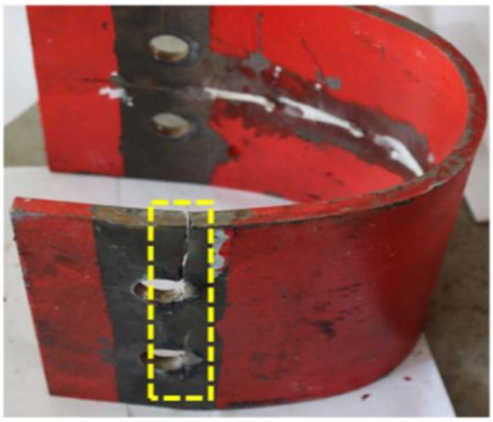

Figure 20: ruptures at bolt holes in sample E transection

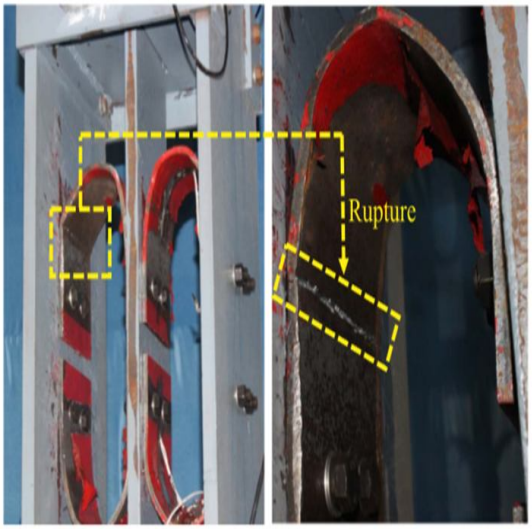

Figure 21: ruptures in sample F's thickness and depth

Hysteretic curves were examined in phase 1 & 2 of the sample tests. Although these samples had different test parameters, the hysteretic curves indicate that all samples indicated favorable cyclic behavior and energy dissipation capacity.

4. Findings

Determining the optimal distance between the two pipes of the proposed damper (8) is among the most significant points, since setting a distance smaller than the proper distance would result in a reduced dissipation capacity for the external pipe (8). In other words, the participation of the internal pipe before creating enough plastic strain in the external pipe will result in an increased damper resistance, making it unable to function as a multilevel system. Besides, setting a distance greater than the proper value will deteriorate the external pipe and ruin the multilevel function. As indicated in Figure 22, increasing the diameter-to-thickness ratio results in an extremely reduced strength and stiffness, leading to an asymmetric hysteresis behavior. Thus, using pipes with low thickness and high diameter-to-thickness ratio increases the chance of buckling and poor performance.

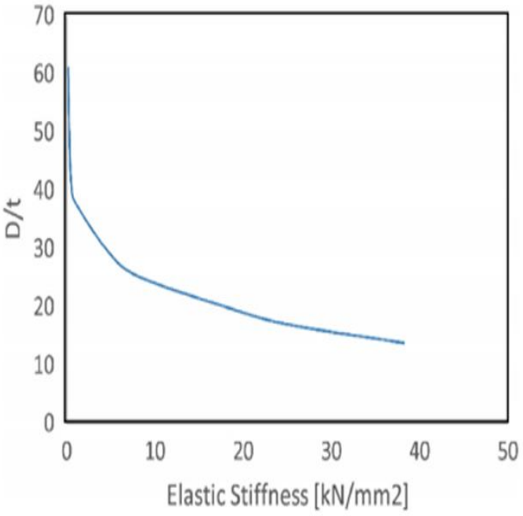

Figure 22: elastic stiffness changes in proportion to D/t

Figure 23 indicates the force-displacement relationship obtained from the cyclic loading test on Naeem et al.'s damper (9). The weak damper yields first while the strong slit dampers remain elastic. As the weal slit damper's displacement reaches 30mm which is slightly smaller than rupture displacement, the slits on the top and bottom of side plates close, transmitting the load to strong slit dampers placed in lower side plates while the weak slit damper prevents further deformation. In this way, slit dampers prevent breaks while remaining active throughout the earthquake. It has been observed that the weal slit section first yields up to 5.3mm displacement, and the load increases again so that strong slit sections yield in a displacement of 38mm. figure 23 also illustrates the dissipated energy, indicating the area in the hysteresis curve increases with the increase of displacement since both slit dampers are active. The side slits closed in a displacement of 30mm during the first cycle of 1.5% relative displacement, but this was due to reasons such as bolt joints slipping, local deformation, and low torsion of the steel plates over the previous loadings, closing the slits over larger displacements in other cycles. Since the deformation of al slit dampers will have ended with the closure of all slits in displacements larger than 60-80mm, the load Increases significantly, and the steel plates act as a steel shear wall.

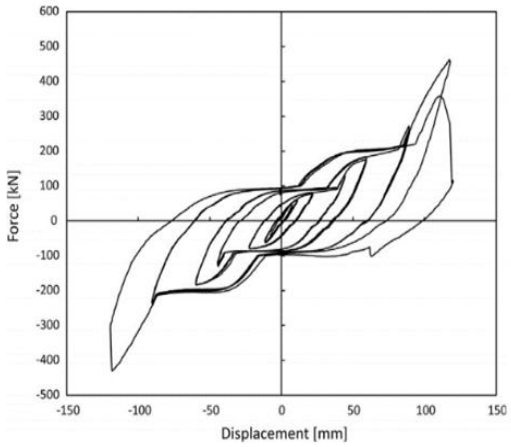

Figure 23: multi-slit damper hysteresis obtained from the loading

In Qu et al.'s (10) damper, All samples indicated stable hysteretic behaviors during the tests. None of the samples showed visible ruptures in the U-shape steel plates in phase 1, except for sample E. along with the increase of displacement, the yield area length increases gradually. Some considerable observations of sample E were made during the last four cycles of phase 1. The web plate centerline of every U-shaped steel plate in sample E did not remain round in the last four cycles of phase 1 due to the stretch and yield actions of the U-shaped steel plates concentrated on the transection consisting of bolt holes. Figure 24 indicates the deformed shape of the U-shaped steel plates in sample E under longitudinal displacements smaller and larger than twice the working flange width (which is 100mm). By the end of phase 1, visible ruptures were observed in sample E in slotted areas where the plate yield was concentrated. No visible rupture was observed in samples G and D over the second phase of the tests, while the U-shaped steel plates of other tested samples ruptured. In samples A and B, the ruptures began in the external surfaces where web plates and flanges met. These ruptures spread towards the inner parts of the U-shaped steel plates due to the gradual return of loading. By the end of phase 2, ruptures

penetrated the depths of the plates but did not reach the full depth of the steel plates in these two samples.

Figures 24 and 25 indicate the hysteretic curves for phase 1 and 2 of the sample tests, respectively. As indicated, although these samples had different test parameters (e.g. geometry, material, bolt hole shapes in the U-shaped steel plates, and loading history), hysteresis curves indicate that all samples have satisfactory cyclic behavior and energy dissipation capacity. All samples except sample C indicated classic bilinear hysteresis response in phase 1 tests. As explained earlier, sample C had the lowest strength, resulting in force measurement becoming unstable during unloading due to test equipment limitations. Although sample C test results do not offer useful information as much as other that of other samples, they indicate the sample's stable resistance in loading and reloading. Therefore, sample C test results have been included to ensure a complete test report. Still, the following sections will focus on other samples in both test phases. Unlike other samples, sample G had bean-shaped bolt holes along four of the 12 U-shaped steel plates.

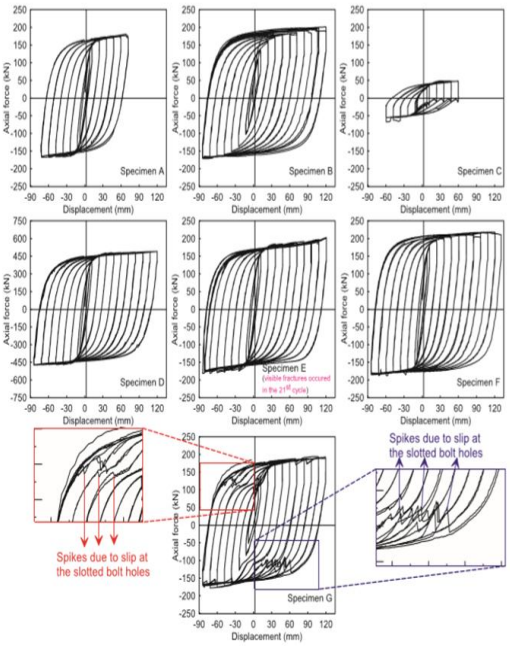

Figure 24: samples' hysteresis curves, phase 1 test results

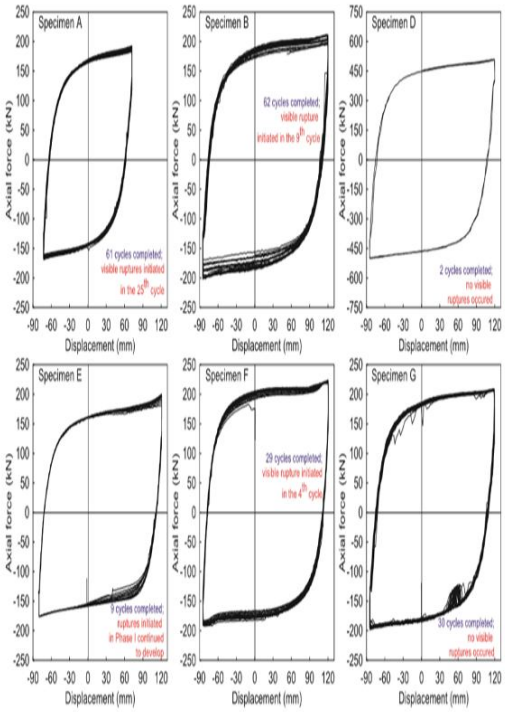

Figure 25: samples' hysteresis curves, phase 2 test results

To examine and compare the frame behaviors with and without U-shaped dampers, nonlinear time history analyses were conducted using a computer program. The nonlinear behaviors of the U-shaped damper and friction damper were modeled by a hardening bilinear elastoplastic shear spring and a bilinear rigid-plastic spring, respectively. To analyze the models' nonlinear dynamics, four different time histories of ground motions were selected. The selected ground motions had various intensities and frequency contents and included a range of Design Basis Earthquakes (DBE) to Maximum Considered Earthquake (MCE) for the site. The selected ground motions include Kobe 1995 (0.35g = PGA), Tabas 1978 (PGA = 0.41g), Northridge 1994 (PGA = 0.56g) and Loma Prieta 1989 (PGA = 0.61g). In total, 72 nonlinear dynamic analyses were performed on three-story, five-story, and ten-story frames under four ground motion time histories. Every frame model without damper was assessed in both normal and

retrofitted with U-shaped and friction dampers design modes.

Analysis results revealed that normal frames are capable of withstanding Kobe and Tabas earthquakes without dampers and through structural members' inelastic behaviors, while they fail under Northridge and Loma Prieta earthquakes. If dampers are added to these frames, they can withstand all four earthquakes through dissipating energy in damper devices instead of main structural members. The retrofitted frames can withstand all four earthquakes through forming plastic hinges in structural elements with no dampers while adding dampers to these frames transmits the inelastic behavior from main structural members to damper members.

Analysis results indicate that placing plastic hinges in normal frame members will not keep any of the three frame models stable under Northridge and Loma Prieta earthquakes without dampers, and the frames will eventually fail. However, the structural member behavior will merely remain elastic by adding either of the two dampers, and plastic deformations will concentrate on damper devices. Failure was not observed in normal frames under Tabas and Kobe earthquake, and retrofitted frames under either of the four earthquake models. Still, many plastic hinges were formed in beams and columns. Again, after adding dampers to the frames, the nonlinear behavior concentrated in the damper and the structural members did not indicate significant inelastic behaviors.

The formation of plastic hinges for five-story retrofitted frames under Loma Prieta and ten-story retrofitted frames under the Kobe earthquake are indicated in Figures 26 and 27. The formation of plastic hinges in frames with and without dampers indicated in these figures will later be compared.

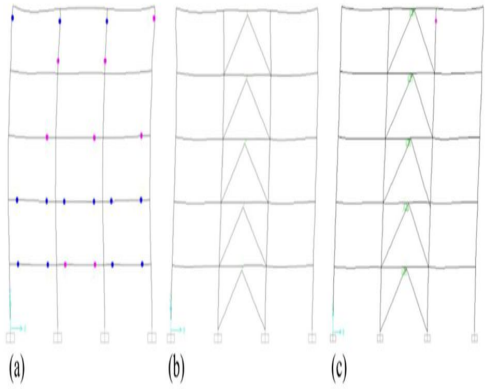

Figure 26: plastic hinges for 5-story retrofitted frames under the Loma Prieta earthquake: a. frame without a damper, b. Frame with U-shaped damper, c. frame with friction damper

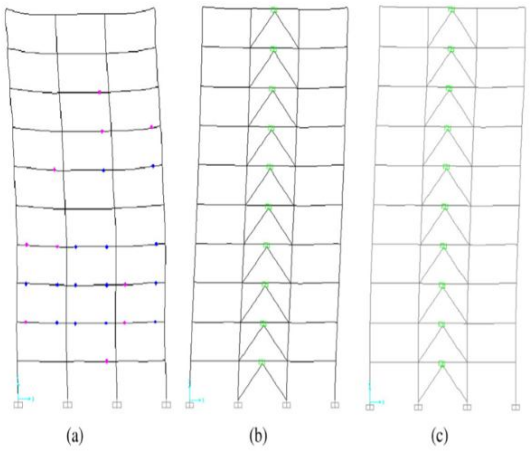

Figure 27: plastic hinges for 10-story retrofitted frames under the Kobe earthquake: a. frame without a damper, b. Frame with U-shaped damper, c. frame with friction damper

5. Conclusions

In paper (8), a new multilevel pipe was introduced in the passive pipe control system and its seismic behavior was analyzed through nonlinear dynamic and static analyses using the finite element method. Given the performed analyses, parameters introduced in the following are suggested to ensure the ductile

behavior in dampers: a diameter-to-thickness ratio of 15-25, a distance between the pipes as large as 0.05-0.07 external pipe diameter, and external pipe diameter to internal pipe diameter ratio of 1.5-2. Also, the damper's bending capacity equivalent force was considered less than the brace's critical buckling force according to the design process, so that no buckling occurs in the braces. The application of the proposed damper will concentrate the failure in pipes, and reduce tension in other structural members. The equivalent viscous damping ratio was calculated to be around 36-50% without the use of complex tools.

It has been observed in the cyclic loading test of the multi-slit damper (9) that two separate yield points exist according to the design, and the damper indicates a stable residual behavior in displacements larger than 4% of the floor height. The force-displacement equation of the test sample obtained from a finite element analysis is consistent with the results obtained from the tests. The analytic model made up of a combination of three nonlinear communication elements has been generated to simulate test results through a structural analysis software. The nonlinear static analysis of the 5-story structure model revealed that a structure retrofitted with the use of the proposed dampers will have a higher ductility capacity during failure compared to those retrofitted with traditional multi-slit dampers. The nonlinear dynamic analysis of the structure model revealed that the average relative displacement within a floor and the average maximum displacement of a retrofitted structure are 36% and 47% less than that of structures retrofitted with the common multi-slit dampers, respectively.

According to experimental and analytic results, it can be inferred that MSD is an effective seismic protection system for frames. It must be mentioned that there is a possibility of a different out-of-plane displacement in the metal plates in MSD when the earthquake results in an intense torsional response in strong structure. Ina high, irregular structure with significant torsional behavior, the metal plate thickness must be increased to prevent large out-of-plane deformation, and the dampers must be placed in a way that eliminates eccentricity and minimalizes the torsional behavior.

Test results (10) indicate that the damper is strong and rupture-resistant in U-shaped steel plates. Many samples continue to dissipate considerable amounts of hysteresis energy even after visible ruptures are observed in U-shaped steel plates. Thus, the damper may be used in future seismic designs.

Empirical studies have revealed that a well-designed damper can be retrofitted after an intense earthquake fast and easily. The retrofitting work only entails the replacement of the U-shaped steel plates which does not require skilled workers. Therefore, the damper can contribute to a flexible and economically convenient seismic design. The thickness of the U-shaped steel plates influences the damper's resistance. Thicker U-shaped steel plates might be used in cases where the damper is expected to have high resistance. However, further research must be conducted to examine the influence of U-shaped steel plates' thickness on the dampers' fatigue life.

Results of nonlinear dynamic analyses revealed that frames without damper are unstable and fail under severe earthquakes (12). However, the inelastic behavior concentrated in the damper device in most cases after the addition of dampers. In the case of retrofitted frames, they could resist all four earthquakes without dampers and through forming plastic hinges in structural parts, while adding dampers to these frames transmitted the inelastic behavior from main structural members to damper members. Both dampers showed proper hysteresis behaviors as well as acceptable plastic deformations in all stories of frames which indicates the proper performance of these dampers in dissipating the input seismic energy. The maximum shear deformation and roof displacement declined across all selected earthquake models after each of the dampers were added. This reduction was in a range of 40-60% base shear force and 13-57% for roof displacement for frames with U-shaped steel plates and 15-41% base shear force and 9-53% for roof displacement for frames with friction dampers.

References

[1] Kelly, J. M.; Skinner, R.; Heine, A., Mechanisms of energy absorption in special devices for use in earthquake resistant structures. *Bulletin of NZ Society for Earthquake Engineering* **1972,** *5* (3), 63-88.

[2] Skinner, R.; Kelly, J.; Heine, A., Hysteretic dampers for earthquake-resistant structures. *Earthquake engineering & structural dynamics* **1974,** *3* (3), 287-296.
[3] Whittaker, A. S.; Bertero, V. V.; G., J. L. A.; Thompson, C., *Earthquake simulator testing of steel plate added damping and stiffness elements*. Earthquake Engineering Research Center, University of California at Berkeley …: 1989; Vol. 89.
[4] Aguirre, M.; Roberto Sanchez, A., Structural seismic damper. *Journal of Structural Engineering* **1992,** *118* (5), 1158-1171.
[5] Dolce, M.; Filardi, B ;.Marnetto, R.; Nigro, D., Experimental tests and applications of a new biaxial elasto-plastic device for the passive control of structures. *Special Publication* **1996,** *164*, 651-674.
[6] Balendra, T.; Yu, C. H.; Lee, F. L., An economical structural system for wind and earthquake loads. *Engineering Structures* **2001,** *23* (5), 491-501.
[7] Zahrai, S.; Vosooq, A., Study of an innovative two-stage control system: Chevron knee bracing & shear panel in series connection. *Structural Engineering and Mechanics* **2013,** *47*.898-881 ,(6)
[8] Cheraghi, A.; Zahrai, S. M., Innovative multi-level control with concentric pipes along brace to reduce seismic response of steel frames. *Journal of Constructional Steel Research* **2016,** *127*, 120-135.
[9] Naeem, A.; Kim, J., Seismic performance evaluation of a multi-slit damper. *Engineering Structures* **2019,** *189*, 332-346.
[10] Qu, B.; Dai, C.; Qiu, J.; Hou, H.; Qiu, C., Testing of seismic dampers with replaceable U-shaped steel plates. *Engineering Structures* **2019,** *179*, 625-639.
[11] Kato, S ;.Kim, Y.-B.; Nakazawa, S.; Ohya, T., Simulation of the cyclic behavior of J-shaped steel hysteresis devices and study on the efficiency for reducing earthquake responses of space structures. *Journal of Constructional Steel Research* **2005,** *61* (10), 1457-1.473
[12] Bagheri, S.; Barghian, M.; Saieri, F.; Farzinfar, A. In *U-shaped metallic-yielding damper in building structures: Seismic behavior and comparison with a friction damper*, Structures, Elsevier: 2015; pp 163-171.
[13] Oh, S.-H.; Kim, Y.-J.; Ryu, H-.S., Seismic performance of steel structures with slit dampers. *Engineering structures* **2009,** *31* (9), 1997-2008.